added 1.0 g (2.8 mmol) of $Cl(n\text{-}Bu)_2SiSi(n\text{-}Bu)_2Cl$ in 5 mL of dry THF, and the solution was refluxed for 22 h. After the usual workup, 1.34 g of crude polymer was obtained as clear viscous liquid.

In an alternate synthesis, the dilithium reagent was prepared from 0.97 g (2.9 mmol) of $HC{\equiv}CSi(n\text{-}Bu)_2Si(n\text{-}Bu)_2C{\equiv}CH$ and 3.65 mL (5.84 mmol) of 1.6 M *n*-BuLi hexane solution, in 20 mL of dry THF. To the dilithium reagent was added 0.52 g (2.8 mmol) of $ClMe_2SiSiMe_2Cl$ in 5 mL of dry THF, and the solution was refluxed for 22 h. After the ususal workup, 1.12 g of crude polymer was obtained as a clear viscous ligand. UV: $\lambda_{max}$ 214 (sh), 226, 240 (sh) nm (THF solution).

**Note Added in Proof.** A recent communication reports the synthesis of polymers similar to these by ring opening of the 8-membered ring dimer: Ishikawa, M.; Hasegawa, Y.; Hatana, T.; Kunai, A. *Organometallics* 1989, *8*, 2741. We have also observed ring-opening polymerization and will report it later.

**Acknowledgment.** This work was supported by the Air Force Office of Scientific Research, Air Force Systems Command, USAF, under Contract No. F49620-86-C-0010.

## References and Notes

(1) (a) Ishikawa, M. *Pure Appl. Chem.* **1978**, *50*, 11. (b) Ishikawa, M.; Kumada, M. *Adv. Organomet. Chem.* **1981**, *19*, 51. (c) Sakurai, H. *J. Organomet. Chem.* **1980**, *200*, 261.

(2) Sakurai, H.; Kira, M.; Sugiyama, H., in press. Sakurai, H. In *Silicon Chemistry*; Corey, J. Y., Corey, E. R., Gaspar, P. P., Eds.; Ellis Horwood Ltd.: Chichester, U.K., 1987.

(3) For an alternate assignment involving $2p\pi$–$3d\pi$ charge transfer see: (a) Shizuka, H.; Obuchi, H.; Ishikawa, M.; Kumada, M. *J. Chem. Soc., Chem. Commun.* **1981**, 405. (b) Shizuka, H.; Sato, Y.; Ishikawa, M.; Kumada, M. *Ibid.* **1982**, 439. (c) Shizuka, H.; Sato, Y.; Ueki, Y.; Ishikawa, M.; Kumada, M. *J. Chem. Soc., Faraday Trans. 1* **1984**, *80*, 341. (d) Shizuka, H.; Obuchi, H.; Ishikawa, M.; Kumada, M. *Ibid.* **1984**, *80*, 383.

(4) Gilman, H.; Atwell, W. H., Schwebke, G. C. *J. Organomet. Chem.* **1946**, *2*, 369.

(5) Sakurai, H.; Kumada, M. *Bull Chem. Soc. Jpn.* **1964**, *37*, 1894.

(6) Sakurai, H.; Nakadaira, Y.; Hosomi, A.; Eriyama, Y.; Kabuto, C. *J. Am. Chem. Soc.* **1983**, *105*, 3359.

(7) (a) Nate, K.; Ishikawa, M.; Ni, H.; Watanabe, H.; Saheki, Y. *Organometallics* **1987**, *6*, 1673. (b) Shinya, K. *J. Organomet. Chem.* **1986**, *310*, C57.

(8) The reaction of the di-Grignard reagents with 1,2-dichlorodisilanes in dilute (0.1 M) THF solution led to the formation of the eight-membered ring disilanyleneacetylene. See: Iwahara, T.; West, R. *J. Chem. Soc., Chem. Commun.* **1988**, *14*, 954.

(9) Sakurai, H.; Tominaga, K.; Watanabe, T.; Kumada, M. *Tetrahedron Lett.* **1966**, *45*, 5493.

(10) Seabald, A.; Seiberlich, P.; Wrackmeyer, B. J. *Organomet. Chem.* **1986**, *303*, 73.

(11) Skattebol, L.; Jones, E. R. H.; Whiting, M. C. *Organic Syntheses*; Wiley: New York, 1963; Collect. Vol. 4, p 792.

**Registry No.** **1a** (SRU), 123438-63-1; **1b** (copolymer), 124755-68-6; **1b** (SRU), 124755-60-8; **1c** (copolymer), 124755-69-7; **1c** (SRU), 124755-61-9; **2b**, 124755-59-5; **3b**, 122202-74-8; **5**, 114953-59-2; **6**, 124755-58-4; $PhSi(Cl)_3$, 98-13-5; *n*-BuLi, 109-72-8; $PhSi(n\text{-}Bu)Cl_2$, 17887-42-2; $PhSi(n\text{-}Bu)_3$, 18510-29-7; $HC{\equiv}CMgBr$, 4301-14-8; $(LiC{\equiv}C(Si(Me)_2)_2C{\equiv}CLi)(Cl(Si(Me)_2)_2Cl)$ (copolymer), 124755-64-2; $(BrC{\equiv}C(Si(Me)_2)_2C{\equiv}CBr)(Cl(Si(Me)_2)_2Cl)$ (copolymer), 124755-66-4.

---

# Normal-Mode Analysis of Infrared and Raman Spectra of Crystalline Isotactic Poly(methyl methacrylate)

**J. Dybal and S. Krimm***,†

*Institute of Macromolecular Chemistry, Czechoslovak Academy of Sciences, 162 06 Prague 6, Czechoslovakia, and Biophysics Research Division and Department of Physics, University of Michigan, Ann Arbor, Michigan 48109.* *Received November 29, 1988;*
*Revised Manuscript Received June 9, 1989*

ABSTRACT: Infrared spectra of oriented and Raman spectra of nonoriented samples of crystalline isotactic poly(methyl methacrylate) (i-PMMA) have been measured. These vibrational spectra have been analyzed by means of normal-mode calculations, using a combined valence force field transferred without refinement from hydrocarbons and from methyl acetate. Calculations have been done for single chain 5/1 and 10/1 helical backbone conformations. Best agreement in the low-frequency region is found between the observed and calculated frequencies for the 10/1 structure. Infrared and Raman bands over the entire spectral region can be satisfactorily interpreted on the basis of the potential energy distributions and dispersion curves for the 10/1 helical conformation of the single i-PMMA chain in the double-stranded structure.

## Introduction

Infrared and Raman spectroscopy, in combination with normal mode calculations, provide a powerful tool for structural analyses of polymers. We present here such a study of the structure and spectrum of isotactic poly(methyl methacrylate) (i-PMMA).

There have been several reports of infrared and Raman spectra and tentative band assignments for (i-PMMA).[1-11] Differently deuterated i-PMMA samples were used in the analyses of the C–H stretch and bend modes.[2,6,7] Bands exhibiting temperature dependences in the infrared spectra of i-PMMA in bulk and in solution were assigned to various conformational forms.[3,8,9] Characteristic solid-state infrared bands of the crystalline and the amorphous phases were determined.[10,11] Using a Urey–Bradley force field refined for polyesters, normal-mode calculations of the low-frequency skeletal modes have been performed on 5/1 helical chain models of i-PMMA.[5] How-

---

† University of Michigan.

0024-9297/90/2223-1301$02.50/0

**Table I**
**Local Symmetry Coordinates for Isotactic Poly(methyl methacrylate)**

| symmetry coordinate | descriptn[a] |
|---|---|
| Alkyl Part | |
| $S_1 = \Delta(r_{15} + r_{52})/(2)^{1/2}$ | CC s1 |
| $S_2 = \Delta(r_{15} - r_{52})/(2)^{1/2}$ | CC s2 |
| $S_3 = \Delta(r_{67} + r_{68} + r_{69})/(3)^{1/2}$ | $\alpha$-$CH_3$ ss |
| $S_4 = \Delta(2r_{67} - r_{68} - r_{69})/(6)^{1/2}$ | $\alpha$-$CH_3$ as2 |
| $S_5 = \Delta(r_{68} - r_{69})/(2)^{1/2}$ | $\alpha$-$CH_3$ as1 |
| $S_6 = \Delta r_{56}$ | $C^\alpha C^\beta$ s |
| $S_7 = \Delta(r_{23} + r_{24})/(2)^{1/2}$ | $CH_2$ ss |
| $S_8 = \Delta(r_{23} - r_{24})/(2)^{1/2}$ | $CH_2$ as |
| $S_9 = \Delta(\theta_{156} + \theta_{152} + \theta_{256} - \theta_{1,5,10} - \theta_{6,5,10} - \theta_{2,5,10})/(6)^{1/2}$ | $CC^\alpha C$ d |
| $S_{10} = \Delta(2\theta_{152} - \theta_{156} - \theta_{256})/(6)^{1/2}$ | $C^\beta$ b1 |
| $S_{11} = \Delta(\theta_{156} - \theta_{256})/(2)^{1/2}$ | $C^\beta$ b2 |
| $S_{12} = \Delta(2\theta_{6,5,10} - \theta_{1,5,10} - \theta_{2,5,10})/(6)^{1/2}$ | C* b1 |
| $S_{13} = \Delta(\theta_{1,5,10} - \theta_{2,5,10})/(2)^{1/2}$ | C* b2 |
| $S_{14} = \Delta(\theta_{768} + \theta_{769} + \theta_{869} - \theta_{567} - \theta_{568} - \theta_{569})/(6)^{1/2}$ | $\alpha$-$CH_3$ sb |
| $S_{15} = \Delta(2\theta_{869} - \theta_{768} - \theta_{769})/(6)^{1/2}$ | $\alpha$-$CH_3$ ab1 |
| $S_{16} = \Delta(\theta_{768} - \theta_{769})/(2)^{1/2}$ | $\alpha$-$CH_3$ ab2 |
| $S_{17} = \Delta(2\theta_{567} - \theta_{568} - \theta_{569})/(6)^{1/2}$ | $\alpha$-$CH_3$ r1 |
| $S_{18} = \Delta(\theta_{568} - \theta_{569})/(2)^{1/2}$ | $\alpha$-$CH_3$ r2 |
| $S_{19} = \Delta(5\theta_{5,2,17} - \theta_{523} - \theta_{524} - \theta_{324} - \theta_{3,12,17} - \theta_{4,2,17})/(30)^{1/2}$ | $C^\alpha CC^\alpha$ d |
| $S_{20} = \Delta(4\theta_{324} - \theta_{523} - \theta_{524} - \theta_{3,2,17} - \theta_{4,2,17})/(20)^{1/2}$ | $CH_2$ b |
| $S_{21} = \Delta(\theta_{523} + \theta_{524} - \theta_{3,2,17} - \theta_{4,2,17})/2$ | $CH_2$ w |
| $S_{22} = \Delta(\theta_{523} - \theta_{524} + \theta_{3,2,17} - \theta_{4,2,17})/2$ | $CH_2$ r |
| $S_{23} = \Delta(\theta_{523} - \theta_{524} - \theta_{3,2,17} + \theta_{4,2,17})/2$ | $CH_2$ t |
| $S_{24} = \Delta\tau_{5,6}$ | $C^\alpha C^\beta$ tor |
| $S_{25} = \Delta\tau_{1,5}$ | $CC^\alpha$ tor |
| $S_{26} = \Delta\tau_{5,2}$ | $C^\alpha C$ tor |
| Ester Part | |
| $S_{27} = \Delta r_{5,10}$ | $C^\alpha C^*$ s |
| $S_{28} = \Delta r_{10,11}$ | CO s |
| $S_{29} = \Delta r_{10,12}$ | C–O s |
| $S_{30} = \Delta r_{12,13}$ | O–C s |
| $S_{31} = \Delta(r_{13,14} + r_{13,15} + r_{13,16})/(3)^{1/2}$ | $OCH_3$ ss |
| $S_{32} = \Delta(2r_{13,14} - r_{13,15} - r_{13,16})/(6)^{1/2}$ | $OCH_3$ as2 |
| $S_{33} = \Delta(r_{13,15} - r_{13,16})/(2)^{1/2}$ | $OCH_3$ as1 |
| $S_{34} = \Delta(2\theta_{5,10,12} - \theta_{5,10,11} - \theta_{11,10,12})/(6)^{1/2}$ | CCO d |
| $S_{35} = \Delta(\theta_{5,10,11} - \theta_{11,10,12})/(2)^{1/2}$ | CO ib |
| $S_{36} = \Delta\pi$ | CO ob |
| $S_{37} = \Delta\theta_{10,12,13}$ | COC d |
| $S_{38} = \Delta(\theta_{14,13,15} + \theta_{14,13,16} + \theta_{15,13,16} - \theta_{12,13,14} - \theta_{12,13,15} - \theta_{12,13,16})/(6)^{1/2}$ | $OCH_3$ sb |
| $S_{39} = \Delta(2\theta_{15,13,16} - \theta_{14,13,15} - \theta_{14,13,16})/(6)^{1/2}$ | $OCH_3$ ab1 |
| $S_{40} = \Delta(\theta_{14,13,15} - \theta_{14,13,16})/(2)^{1/2}$ | $OCH_3$ ab 2 |
| $S_{41} = \Delta(2\theta_{12,13,14} - \theta_{12,13,15} - \theta_{12,13,16})/(6)^{1/2}$ | $OCH_3$ r1 |
| $S_{42} = \Delta(\theta_{12,13,15} - \theta_{12,13,16})/(2)^{1/2}$ | $OCH_3$ r2 |
| $S_{43} = \Delta\tau_{10,12}$ | C*–O tor |
| $S_{44} = \Delta\tau_{12,13}$ | O–C tor |
| $S_{45} = \Delta\tau_{5,10}$ | $C^\alpha C^*$ tor |

[a] Abbreviations: s, stretch; as, antisymmetric stretch; ss, symmetric stretch; b, bend; ab, antisymmetric bend; sb, symmetric bend; ib, in-plane bend; ob, out-of-plane bend; d, deformation; r, rock; w, wag; t, twist; tor, torsion.

**Table II**
**Force Constants for Isotactic Poly(methyl methacrylate)**

| force const | value[c] |
|---|---|
| Alkyl Part:[a] C–$CH_3$ Group | |
| *f*(CH) | 4.699 |
| *f*(HCH) | 0.540 |
| *f*(CCH) | 0.645 |
| *f*(CH′,CH″) | 0.043 |
| *f*(CCH′,CCH″) | −0.012 |
| *f*($C^\alpha$–$C^\beta$ torsion) | 0.072 |
| Alkyl Part:[a] C–$CH_2$–C Group | |
| *f*(CH) | 4.554 |
| *f*(HCH) | 0.550 |
| *f*(CCH) | 0.656 |
| *f*(CCC) | 1.130 |
| *f*(CH′,CH″) | 0.006 |
| *f*(CCH′,CCH″) | −0.021 |
| *f*(HCC′,CC″) | 0.079 |
| *f*(HCC′,HCC″) | 0.012 |
| *f*(HCC,CCC′) | −0.031 |
| Alkyl Part:[a] Rest of Force Constants | |
| *f*(CC) | 4.337 |
| *f*(CCC) | 1.086 |
| *f*(C–C torsion) | 0.024 |
| *f*(CC′,CC″) | 0.101 |
| *f*(CC,CCH) | 0.328 |
| *f*(CC,CCC′) | 0.417 |
| *f*(CCC′,CCC″) | −0.041 |
| *f*(HCC,CCC′-trans) | 0.049 |
| *f*(HCC,CCC′-gauche) | −0.052 |
| *f*(C′CC,CCC″-trans) | −0.011 |
| *f*(C′CC,CCC″-gauche) | 0.011 |
| Ester Part[b] | |
| *f*(27,27) | 4.046 |
| *f*(28,28) | 11.009 |
| *f*(29,29) | 5.031 |
| *f*(30,30) | 5.062 |
| *f*(31,31) | 5.050 |
| *f*(32,32) | 4.859 |
| *f*(33,33) | 4.789 |
| *f*(34,34) | 1.129 |
| *f*(35,35) | 1.259 |
| *f*(36,36) | 0.734 |
| *f*(37,37) | 1.729 |
| *f*(38,38) | 0.661 |
| *f*(39,39) | 0.485 |
| *f*(40,40) | 0.518 |
| *f*(41,41) | 0.868 |
| *f*(42,42) | 0.835 |
| *f*(43,43) | 0.210 |
| *f*(44,44) | 0.032 |
| *f*(45,45) | 0.024 |
| *f*(28,29) | 0.971 |
| *f*(27,28) | 0.971 |
| *f*(30,32) | −0.639 |
| *f*(29,30) | 0.731 |
| *f*(29,35) | −0.219 |
| *f*(27,35) | 0.219 |

[a] Force constants in terms of internal coordinates. [b] Force constants in terms of local symmetry coordinates of Table I. [c] Units are mdyn/Å for stretch and stretch, stretch force constants, mdyn for stretch, bend force constants, and mdyn Å for all others.

ever, there has as yet been no definitive, full interpretation of the vibrational spectra of i-PMMA.

In this paper we present further experimental studies and the results of normal-mode calculations of i-PMMA. We have measured the infrared and Raman spectra of partially crystalline i-PMMA, prepared by annealing solid samples.[5,12,13] Polarized infrared spectra of oriented and Raman spectra of nonoriented crystalline i-PMMA samples have been obtained. In the normal-mode calculations, we used valence force constants refined for branched hydrocarbons[14] and for methyl acetate.[15]

The structure of i-PMMA has been the subject of controversy. Stroupe and Hughes[16] proposed a 5/2 helix, but subsequent X-ray[17] and X-ray plus far infrared and normal mode[5] studies suggested a 5/1 helical backbone conformation. After an intramolecular energy calculation indicated that a 12/1 helix chain was more stable than a 5/1 helix,[18] the X-ray pattern was reexamined and found to be more consistent with a double helix of 10/1 chains.[19] This was subsequently disputed on the basis of X-ray studies of crystalline[20] and noncrystalline[21] i-PMMA. However, the 10/1 helix structure has been supported by virtual bond[22] and conformational energy[23,24] calculations and by a combined X-ray diffraction and energy calculation study.[25]

**Table III**
**Observed and Calculated Frequencies ($cm^{-1}$) of Selected Vibrations of Isotactic Poly(methyl methacrylate)**

| obsd | | | calcd | | | | |
|---|---|---|---|---|---|---|---|
| infrared[a] | | | 10/1 helix | | 5/1 helix | | potential energy distributn[b] 5/1 helix |
| ‖ | ⊥ | Raman | A | $E_1$ | A | $E_1$ | |
| 1268 | | | 1252 | | 1266 | | $CH_2$ t(41), CC s1(14) |
| 1198 | | | 1202 | | 1212 | | C–O s(20), $CH_2$ w(12) |
| 1154 | | 1150 | 1147 | | 1170 | | $CH_2$ t(23), $\alpha$-$CH_3$ r1(16), CC s1(13) |
| | 1115 | | | 1127 | | 1090 | $\alpha$-$CH_3$ r1(22), $CH_2$ t(19), $C^{\alpha}C^{\beta}$ s(16) |
| | 932 | | | 954 | | 940 | $CH_2$ r(26), $\alpha$-$CH_3$ r1(22), CC s2(13) |
| | 846 | | | 854 | | 864 | $CH_2$ r(17), $C^{\alpha}C$ s(15), $C^{\alpha}C^*$ s(13) |
| | 609<br>559 | | | 603 | | 637 | $C^{\alpha}C^*$ s(21), CO ib(17), $CC^{\alpha}C$ d(13) |
| 559 | | 597<br>562 | 602 | | 627 | | $C^{\alpha}C^*$ s(26), CO ib(20), $CC^{\alpha}C$ d(13) |
| | 480 | 481 | | 466 | | 484 | CCO d(16), CC s1(14) |
| 476 | | | 467 | | 464 | | CCO d(21), $C^*$ b1(17) |
| | 406 | 390 | | 380 | | 443 | $C^{\beta}$ b2(21), $CC^{\alpha}C$ d(13) |
| 365 | | 372 | 366 | | 391 | | $C^{\beta}$ b2(30), $CC^{\alpha}C$ d(11) |
| | 368 | | | 345 | | 355 | COC d(23), $C^{\beta}$ b2(13), $C^*$ b1(21) |
| | | 341 | 335 | | 338 | | COC d(33), CO ib(25), $C^*$ b1(21) |
| | 338 | | | 325 | | 339 | CO ib(25), COC d(23), $C^*$ b1(20) |
| 314 | | 314 | 309 | | 295 | | $CC^{\alpha}C$ d(31), $C^*$ b2(11) |
| | 232 | | | 252 | | 273 | $CC^{\alpha}C$ d(25), $C^{\beta}$ b2(20) |
| | | 221 | 235 | | 261 | | $C^*$ b2(27), C–O tor(21), $C^{\beta}$ b2(21) |
| 217 | | | 206 | | 201 | | $C^*$ b1(20), $C^{\alpha}C^*$ tor(19), $C^{\beta}$ b2(17) |

[a] Infrared bands: ‖, parallel dichroism; ⊥, perpendicular dichroism. [b] Abbreviations: s, stretch; b, bend; ib, in-plane bend; d, deformation; r, rock; w, wag; t, twist; tor, torsion. Only contributions 10% or greater are included.

Distinctions between different local conformations of a regular polymer chain can be made on the basis of normal-mode analyses of the vibrational spectrum, since the infrared and Raman bands, particularly in the low-frequency region, are sensitive to the three-dimensional arrangement of the atoms. This has been amply demonstrated on macromolecules as diverse as polyethylene,[26] poly(vinyl chloride),[27] and polypeptides.[28] We have used the same approach here, calculating the normal modes of the 5/1 and 10/1 helical structures of i-PMMA and comparing these predictions with the observed bands for the crystalline polymer. Since the force fields used in the calculations[14,15] have proven to be highly successful in accounting for observed spectra of related molecules, we can expect the predictions for i-PMMA to result in meaningful distinctions in structure. This is the case, with the 10/1 helical conformation being clearly favored. We discuss this determination first and then present a more detailed analysis of the spectrum of the 10/1 helix structure.

## Experimental Section

The sample of isotactic PMMA used in the present study was kindly supplied by Dr. R. O. Loutfy from Xerox Research Center of Canada. The tacticity of the polymer sample was determined on the basis of proton NMR spectra: the content of isotactic triads is higher than 98%.[29]

Films of i-PMMA were prepared by casting of toluene solutions on an aluminum foil and subsequent room-temperature evaporation of the solvent. Samples for Raman measurements consisted of about fifty layers of such films. For infrared measurements, oriented samples were obtained by stretching the films (in water at 50 °C) 10–15 times their original length. Crystallinity was induced by then annealing in a vacuum oven at 120 °C for 8 days. This temperature is optimum with respect to the crystallization rate.[12,13] Polarized infrared spectra were obtained with the electric vector parallel and perpendicular to the stretching direction. No polarization results are available for the Raman spectra because the sample used in the measurements had no defined orientation.

Raman spectra were obtained with a Spex 1403 double monochromator equipped with holographic gratings. Spectra were excited by the 514.5-nm line of a Coherent Radiation 52 argon ion laser, and 90° scattering geometry was used. Infrared spectra were recorded on a Bomem DA3 FTIR spectrometer.

## Normal-Mode Calculations

The normal-mode calculations were done on regular single chain 5/1[5] and 10/1[19] helical structures. This is a reasonable approximation, since the interchain forces are weak in comparison to the intrachain; though they may determine the chain conformation, they do not influence its frequencies significantly (possibly giving rise to small band shifts and/or splittings). The specific three-dimensional structure that results from these interactions is primarily responsible for its characteristic frequency distribution.

The following structural parameters (bond lengths and bond angles) were used in the normal-mode calculations: $CC^{\alpha} = C^{\alpha}C = C^{\alpha}C^{\beta} = 1.53$ Å, $C^{\alpha}C^* = 1.51$ Å, CH = 1.09 Å, $C^*O^* = 1.21$ Å, $C^*O = 1.34$ Å, OC = 1.46 Å, $C^{\alpha}C^*O^* = 127°$, $C^{\alpha}C^*O = 122°$, $C^*OC = 117°$. The ester group was assumed to be in a planar conformation. The bond lengths and bond angles of the ester group were taken from the results of the ab initio optimization of the methyl acetate molecular geometry.[30] The bond angles in both the ester and $\alpha$-methyl groups were assumed to be tetrahedral. According to the results of the X-ray studies[5,19] and the conformational energy calculations,[23,24] both bond angles in the chain backbone are appreciably distorted relative to the tetrahedral value. In the present calculations, however, the main-chain angles were kept tetrahedral in order to ensure transferability of the force constants. Cartesian coordinates were calculated for the ideal 5/1 and 10/1 helical structures of the isolated i-PMMA chain, with alternating skeletal torsion angles of 0° and 72° and of 0° and 36°, respectively. All the ester groups were assumed to be parallel, with the $OCH_3$ group oriented trans with respect to the $\alpha$-$CH_3$ group. The symmetry coordinates, constructed from the internal coordinates defined in the standard way, are listed in Table I with the numbering of atoms shown in Figure 1.

The optically active modes of an infinite, isolated i-PMMA chain with helical conformation are classified into

**Table IV**
**Observed and Calculated Frequencies ($cm^{-1}$) of Isotactic Poly(methyl methacrylate)**

| obsd | | | calcd | | | |
|---|---|---|---|---|---|---|
| infrared[a] | | | | | | |
| ∥ | ⊥ | Raman | A | $E_1$ | $E_2$ | potential energy distributn[b] |
| 3029 | | 3027 | 3025 | 3025 | 3025 | $OCH_3$ as2(99) |
| 3005 | 3005 | 3006 | 3002 | 3002 | 3002 | $OCH_3$ as1(99) |
| | | | 2961 | | | $\alpha$-$CH_3$ as2(96) |
| | | | | 2961 | | $\alpha$-$CH_3$ as2(80), $\alpha$-$CH_3$ as1(20) |
| | | | | | 2961 | $\alpha$-$CH_3$ as1(54), $\alpha$-$CH_3$ as2(45) |
| 2955 | 2954 | 2953 | 2961 | | | $\alpha$-$CH_3$ as1(96) |
| | | | | 2961 | | $\alpha$-$CH_3$ as1(80), $\alpha$-$CH_3$ as2(20) |
| | | | | | 2961 | $\alpha$-$CH_3$ as2(54), $\alpha$-$CH_3$ as1(45) |
| | | | 2961 | 2961 | 2961 | $OCH_3$ ss(100) |
| 2912 | 2914 | 2919 | 2928 | 2928 | 2928 | $CH_2$ as(99) |
| 2880 | 2880 | | 2882 | 2882 | 2882 | $\alpha$-$CH_3$ ss(100) |
| 2841 | 2840 | 2842 | 2856 | 2856 | 2856 | $CH_2$ ss(99) |
| 1733 | 1736 | 1738,1725 | 1749 | 1749 | 1749 | CO s(82), CCO d(10) |
| 1486 | | 1486 | 1473 | | | $CH_2$ b(54), $\alpha$-$CH_3$ ab1(34) |
| | 1486 | | | 1472 | | $CH_2$ b(47), $\alpha$-$CH_3$ ab1(40) |
| | | | | | 1470 | $\alpha$-$CH_3$ ab1(54), $CH_2$ b(33) |
| | | | 1467 | | | $\alpha$-$CH_3$ ab2(90) |
| | | | | 1467 | | $\alpha$-$CH_3$ ab2(89) |
| | | | | | 1467 | $\alpha$-$CH_3$ ab2(85) |
| | | | 1462 | | | $\alpha$-$CH_3$ ab1(55), $CH_2$ b(39) |
| | | | | 1462 | | $\alpha$-$CH_3$ ab1(48), $CH_2$ b(45) |
| | | | | | 1461 | $CH_2$ b(63), $\alpha$-$CH_3$ ab1(30) |
| 1454 | 1453 | | 1456 | 1456 | 1456 | $OCH_3$ ab2(84), $OCH_3$ r2(16) |
| 1442 | 1442 | 1447 | 1445 | 1445 | 1445 | $OCH_3$ sb(95) |
| 1432 | 1433 | 1432 | 1426 | 1426 | 1426 | $OCH_3$ ab1(72), $OCH_3$ r1(24) |
| | | | | | 1392 | $\alpha$-$CH_3$ sb(69) |
| | 1386 | | | 1390 | | $\alpha$-$CH_3$ sb(76) |
| 1386 | | 1388 | 1389 | | | $\alpha$-$CH_3$ sb(78) |
| | | | | | 1337 | $\alpha$-$CH_3$ sb(25), $CH_2$ w(21), $C^{\alpha}C^*$ s(17), $CH_2$ t(13) |
| | 1338 | 1335 | | 1329 | | $CH_2$ w(34), CC s2(19), $\alpha$-$CH_3$ sb(16), $C^{\alpha}C^*$ s(15) |
| 1329 | | | 1325 | | | $CH_2$ w(39), CC s2(25), $C^{\alpha}C^*$ s(14), $\alpha$-$CH_3$ sb(14) |
| | | | | | 1325 | $CH_2$ w(47), CC s2(32) |
| | 1298 | | | 1315 | | CC s2(32), $CH_2$ w(29), $C^{\alpha}C^*$ s(14) |
| 1296 | | | 1310 | | | CC s2(31), $CH_2$ w(23), $C^{\alpha}C^*$ s(15), C–O s(12) |
| | | | | | 1267 | CC s1(22), $C^{\alpha}C^{\beta}$ s(12), CC s2(12) |
| | 1252 | | | 1259 | | CC s1(24), $CH_2$ t(15), $C^{\alpha}C^{\beta}$ s(13), $C^{\alpha}CC^{\alpha}$ d(10) |
| 1268 | | 1270 | 1252 | | | CC s1(28), $CH_2$ t(22), $C^{\alpha}C^{\beta}$ s(14), $C^{\alpha}CC^{\alpha}$ d(12) |
| | | 1231 | | | 1231 | C–O s(27), $CH_2$ t(26), CO ib(11) |
| | 1198 | | | 1208 | | $CH_2$ t(21), C–O s(18), $OCH_3$ r1(14) |
| 1198 | | | 1202 | | | $OCH_3$ r1(24), C–O s(16), $OCH_3$ ab1(11) |
| 1190 | | 1190 | 1192 | | | $CH_2$ t(26), $CH_2$ w(19), $OCH_3$ r1(13) |
| | 1190 | | | 1188 | | $OCH_3$ r1(33), $CH_2$ t(20), $OCH_3$ ab1(11) |
| | | | | | 1187 | $OCH_3$ r1(47), $OCH_3$ ab1(16), COC d(11) |
| | | | 1178 | | | $CH_2$ t(36), $OCH_3$ r1(17) |
| | 1150 | | | 1177 | | $CH_2$ w(17), $CH_2$ t(14), $\alpha$-$CH_3$ r1(12) |
| | | 1157 | | | 1156 | $CH_2$ w(19), $\alpha$-$CH_3$ r2(16), CC s2(11), $CH_2$ t(11) |
| 1154 | | 1150 | 1147 | | | $C^{\alpha}C^{\beta}$ s(14), $CH_2$ w(13), $CH_2$ t(13), O–C s(10) |
| | | 1123 | | 1129 | | $OCH_3$ r2(51), $OCH_3$ ab2(10) |
| | | | | | 1128 | $OCH_3$ r2(82), $OCH_3$ ab2(16) |
| 1115 | | 1113 | 1128 | | | $OCH_3$ r2(82), $OCH_3$ ab2(16) |
| | 1115 | | | 1127 | | $OCH_3$ r2(32), $CH_2$ t(12) |
| | | | | | 1100 | $CH_2$ t(22), $CH_3$ r1(17), $C^{\alpha}C^{\beta}$ s(16), O–C s(11) |
| 998 | | 996 | 1036 | | | O–C s(77), $OCH_3$ r1(10) |
| | 998 | | | 1036 | | O–C s(76), $OCH_3$ r1(10) |
| | | | | | 1034 | O–C s(71), $OCH_3$ r1(10) |
| 951 | | | 969 | | | $\alpha$-$CH_3$ r1(54), $CH_2$ r(21) |
| | | 960 | | | 968 | $\alpha$-$CH_3$ r2(34), $\alpha$-$CH_3$ r1(23), CC s2(15), $CH_2$ r(12) |
| | 953 | 953 | | 966 | | $\alpha$-$CH_3$ r1(48), $CH_2$ r(21) |
| | 932 | 931 | | 954 | | $\alpha$-$CH_3$ r2(51), CC s2(30) |
| 937 | | | 952 | | | $\alpha$-$CH_3$ r2(59), CC s2(32) |
| | | | | | 946 | CC s2(20), $\alpha$-$CH_3$ r1(20), $\alpha$-$CH_3$ r2(18), $CH_2$ r(16) |
| | | | | | 860 | $C^{\alpha}C^{\beta}$ s(22), $CH_2$ r(15), $C^{\alpha}C^*$ s(14), C–O s(13) |
| | 846 | | | 854 | | $C^{\alpha}C^{\beta}$ s(24), $CH_2$ r(17), C–O s(14), $C^{\alpha}C^*$ s(13) |
| 843 | | 844 | 853 | | | $C^{\alpha}C^{\beta}$ s(26), $CH_2$ r(18), C–O s(14), $C^{\alpha}C^*$ s(12) |
| 810 | | 809 | 804 | | | $C^{\alpha}C^{\beta}$ s(24), C–O s(10) |
| | 808 | | | 803 | | $C^{\alpha}C^{\beta}$ s(23), C–O s(10) |
| | | | | | 800 | $C^{\alpha}C^{\beta}$ s(19), C–O s(10) |
| | | 782 | | | 778 | CO ob(52), $C^*$ b2(11) |
| | 764 | | | 772 | | CO ob(61), $C^*$ b2(12) |
| 758 | | 764 | 770 | | | CO ob(64), $C^*$ b2(12) |
| | | | | | 606 | $C^{\alpha}C^*$ s(26), CO ib(18), $CC^{\alpha}C$ d(10) |
| | 609<br>559 | | | 603 | | $C^{\alpha}C^*$ s(30), CO ib(21) |

**Table IV (Continued)**

| obsd | | | | | | |
|---|---|---|---|---|---|---|
| infrared[a] | | | calcd | | | |
| ∥ | ⊥ | Raman | A | $E_1$ | $E_2$ | potential energy distributn[b] |
| 559 | | 597<br>562 | 602 | | | $C^{\alpha}C^{*}$ s(31), CO ib(22) |
| | | | | | 481 | CC s1(22), CCO d(11) |
| | 480 | 481 | | 466 | | CCO d(22), $CC^{\alpha}C$ d(19), $C^{*}$ b1(16) |
| 476 | | | 467 | | | $CC^{\alpha}C$ d(22), CCO d(21), $C^{*}$ b1(17), $CH_2$ r(12) |
| | | 464 | | | 455 | $CC^{\alpha}C$ d(17), CCO d(12), $C^{\beta}$ b2(10) |
| | 406 | 390 | | 380 | | $C^{\beta}$ b2(27), $C^{*}$ b2(12), $CC^{\alpha}C$ d(10) |
| 365 | | 372 | 366 | | | COC d(25), $CC^{\alpha}C$ d(16), $C^{*}$ b2(15) |
| | | | | | 359 | COC d(24), $CC^{\alpha}C$ d(16), $C^{\beta}$ b2(13) |
| | 368 | | | 345 | | COC d(36), CO ib(15), $C^{*}$ b1(10) |
| | | | | | 337 | CO ib(25), COC d(22), $C^{*}$ b1(19) |
| | | 341 | 335 | | | CO ib(21), $C^{*}$ b1(21), COC d(20) |
| | 338 | | | 325 | | $CC^{\alpha}C$ d(30), $C^{*}$ b1(15), CO ib(12) |
| 314 | | 314 | 309 | | | $C^{\beta}$ b2(32), $CC^{\alpha}C$ d(21) |
| | | | | | 268 | $C^{\beta}$ b2(32), $CC^{\alpha}C$ d(17), $C^{*}$ b1(14), $C^{\beta}$ b1(10) |
| | 232 | | | 252 | | $C^{\beta}$ b2(39), $C^{*}$ b2(13), C–O tor(11) |
| | | 221 | 235 | | | C–O tor(34), $C^{\beta}$ b2(25), $C^{*}$ b2(24) |
| 217 | | | 206 | | | CCO d(36), $C^{*}$ b1(35), COC d(11) |
| | | | | 202 | | $C^{\alpha}C^{\beta}$ tor(30), CCO d(21), $C^{*}$ b1(19), C–O tor(12) |
| | | | | | 201 | $C^{\alpha}C^{\beta}$ tor(33), CCO d(17), C–O tor(11) |
| | | | | | 197 | $C^{\alpha}C^{\beta}$ tor(50), C–O tor(18) |
| | | | 195 | | | $C^{\alpha}C^{\beta}$ tor(97) |
| | 188 | | | 193 | | $C^{\alpha}C^{\beta}$ tor(70), CCO d(10) |
| | | | | | 185 | C–O tor(29), CCO d(16), $C^{\alpha}C^{\beta}$ tor(16), $C^{*}$ b1(14) |
| | | | | 164 | | C–O tor(25), O–C tor(21) |
| 165 | | | 144 | | | O–C tor(65), $C^{*}$ b2(17) |
| | | | | | 133 | O–C tor(62) |
| | 140 | | | 128 | | O–C tor(68), C–O tor(17) |
| | | | | | 115 | $C^{\beta}$ b1(20), O–C tor(19), C–O tor(16), $C^{\alpha}CC^{\alpha}$ d(15) |
| 109 | | | 110 | | | C–O tor(41), O–C tor(29), $C^{\alpha}$ b2(18) |
| | 113 | | | 86 | | $C^{*}$ b2(29), $C^{\beta}$ b1(16), $C^{\alpha}C^{*}$ tor(15) |
| | | 85 | 72 | | | CC s1(36), $C^{\beta}$ b1(27), $C^{\alpha}CC^{\alpha}$ d(11) |
| | | | | | 71 | $C^{\alpha}CC^{\alpha}$ d(28), $C^{*}$ b2(24), $C^{\alpha}C^{*}$ tor(15) |
| | | | | 47 | | $C^{\alpha}CC^{\alpha}$ d(39), $C^{\alpha}C^{*}$ tor(23), $C^{\beta}$ b1(22) |
| | | | 44 | | | $C^{\alpha}C^{*}$ tor(88) |
| | | | | | 39 | $C^{\alpha}C^{*}$ tor(75) |
| | | | | 36 | | $C^{\alpha}C^{*}$ tor(58), $C^{\alpha}CC^{\alpha}$ d(12) |
| | | | 24 | | | $C^{\alpha}CC^{\alpha}$ d(55), $C^{\beta}$ b1(35) |
| | | | | | 17 | $C^{\alpha}C$ tor(58), $CC^{\alpha}$ tor(27) |
| | | | | 8 | | $C^{\alpha}C$ tor(45), $CC^{\alpha}$ tor(38) |
| | | | | | 7 | $CC^{\alpha}$ tor(53), $C^{\alpha}C$ tor(24) |

[a] Infrared bands: ∥, parallel dichroism; ⊥, perpendicular dichroism. [b] Abbreviations: s, stretch; as, antisymmetric stretch; ss, symmetric stretch; b, bend; ab, antisymmetric bend; sb, symmetric bend; ib, in-plane bend; ob, out-of-plane bend; d, deformation; r, rock; w, wag; t, twist; tor, torsion. Only contributions 10% or greater are included.

A, $E_1$, and $E_2$ symmetry species, where the phase differences between the motions in adjacent monomer units are 0°, 72°, and 144° for the 5/1 helix and 0°, 36°, and 72° for the 10/1 helix, respectively. The former two species are both infrared and Raman active, and the last is Raman active only. In the infrared dichroic spectrum, the A modes are polarized parallel and the $E_1$ modes perpendicular to the helix axis.

The force constants for the aliphatic chain were taken to be those determined by Snyder and Schachtschneider for branched hydrocarbons.[14] The force constants for the ester group were taken directly from our work on methyl acetate.[15] Using this combined force field, we obtained good agreement between the observed frequencies of i-PMMA and those calculated for the 10/1 helical structure. A tentative refinement of specific force constants by a least-squares iteration did not significantly improve the overall fit between the observed and calculated frequencies. Therefore, rather than undertake a refinement based on the assumed geometry, the combined valence force fields transferred from hydrocarbons and methyl acetate (listed in Table II) were used without modification in the normal-mode analysis of i-PMMA. This permits one to have greater confidence in the results of the calculations, which provide practically complete assignments for the observed vibrational spectra, even though the frequency agreement in some cases is poor.

## Results and Discussion

Raman spectra of the annealed i-PMMA sample (partially crystalline) and of the sample prepared by solvent evaporation without annealing (amorphous) are shown in Figure 2. Several differences can be observed between the spectra of crystalline and amorphous i-PMMA, which are characteristic of a transition from unordered to ordered polymer. The bands in the spectrum of crystalline i-PMMA are much sharper and many of them exhibit frequency shifts and changes in intensity, e.g., the peaks in regions 1200–1000 $cm^{-1}$ and 1000–900 $cm^{-1}$. In the spectrum of the crystalline form, a new band at 314 $cm^{-1}$ is observed that does not appear in the spectrum of the amorphous form. The mode near 372 $cm^{-1}$ is observed to split into two components in the spectrum of the crystalline sample, at 372 and 390 $cm^{-1}$. The band at 1729 $cm^{-1}$, corresponding to the C=O stretch vibration, is also split in the spectrum of the crystalline form, into a doublet at 1738 and 1725 $cm^{-1}$ (clearly visible in expanded

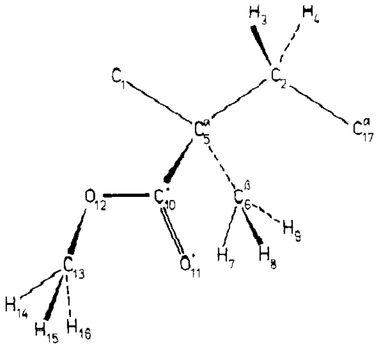

**Figure 1.** Structural unit of i-PMMA, with atom numbering.

spectra). Analogous splittings of the C=O stretch mode have been observed previously in the spectra of the ordered structures of syndiotactic PMMA.[31]

Differences in the infrared spectra between amorphous and partially crystalline samples have been discussed previously.[10,11] Bands characteristic of the amorphous phase were found at 1047 and 938 $cm^{-1}$, while characteristic bands of the crystalline phase were found at 1338, 1298, and 882 $cm^{-1}$. Polarized infrared spectra of the annealed oriented (partially crystalline) i-pMMA film are shown in Figure 3.

Some observed infrared and Raman frequencies are listed in Table III and compared with calculated frequencies of the 5/1 and 10/1 helical structures. In this table we list only the A and $E_1$ species modes above 600 $cm^{-1}$ for which the calculated frequencies differ by 10 $cm^{-1}$ or more and all the modes in the 600–200 $cm^{-1}$ region. Experience has shown[5,32] that the low-frequency region is most sensitive to small changes in conformation of the chain backbone. (The $E_2$ species modes are not listed here since the assignments of low-frequency Raman bands to this species are less certain.)

As can be seen from Table III, the calculated frequencies of the 10/1 helix are in better agreement with the observed bands than are those of the 5/1 helix. The average difference between observed and calculated frequencies is 21.1 $cm^{-1}$ for the 5/1 helix compared to 12.8 $cm^{-1}$ for the 10/1 helix (the average difference for this helix over the spectral range of 1800–85 $cm^{-1}$ is 11.6 $cm^{-1}$). Although there are some large discrepancies in the latter case, these results clearly show that the 10/1 helix is in better agreement with the observed infrared and Raman data than is the 5/1 helix. They thus provide additional support for this model of the chain conformation in the crystal structure of i-PMMA.

We turn now to a detailed analysis of the spectra of crystalline i-PMMA based on the 10/1 helix model of the chain conformation. The observed infrared and Raman band frequencies are listed in Table IV together with the calculated A, $E_1$, and $E_2$ normal-mode frequencies and potential energy distributions (PED). The experimental infrared frequencies in the region below 600 $cm^{-1}$ are taken from the paper of Tadokoro et al.[5] Band assignments have been made on the basis of extensive spectral studies of isotopic derivatives of i-PMMA[2,6,7] as well as our infrared dichroism results. Since it is often difficult to assign Raman bands to specific species, we have in such cases associated the band with the A species mode. Dispersion curves are given in Figure 4.

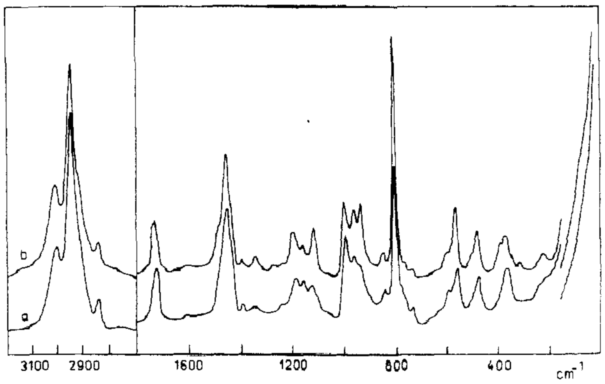

**Figure 2.** Raman spectra of i-PMMA: (a) amorphous sample; (b) partially crystalline sample.

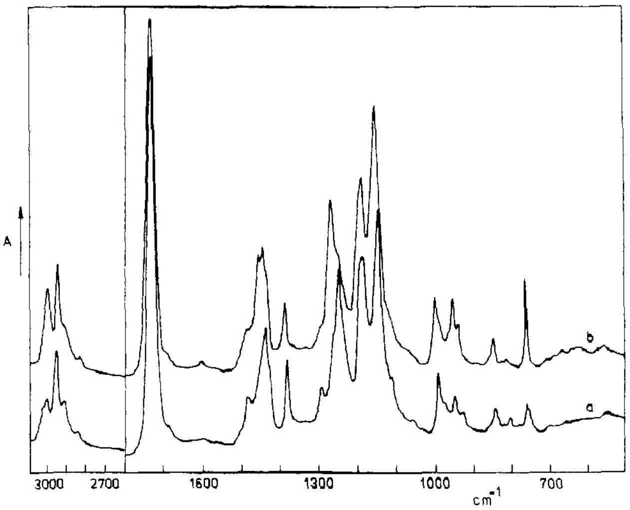

**Figure 3.** Polarized infrared spectra of oriented sample of partially crystalline i-PMMA, measured with the electric vector (a) perpendicular and (b) parallel to the draw direction.

The bands in the C–H stretch region, from 3100 to 2800 $cm^{-1}$, are probably affected by Fermi resonance between the C–H stretch fundamentals and overtones and combinations of lower frequency modes, which complicate the band assignments.[2,6,7,33] However, as can be seen from Table IV, the results of the normal-mode calculations suggest a reasonable interpretation of the observed bands in this region that is in qualitative agreement with the conclusions of studies of specifically deuterated derivatives of i-PMMA.[6,7]

The splitting of the C=O stretch mode near 1730 $cm^{-1}$, observed in the spectra of crystalline i-PMMA, is not reproduced in our normal mode calculation of the isolated *i*-PMMA chain (Table IV). We believe that this splitting can be explained by resonance transition dipole interactions, which were not included in the calculations. This is similar to the observed splittings of the amide I and amide II modes in polypeptides[34-36] and the C=O stretch splitting in acid dimers,[34,37] both of which are satisfactorily reproduced when such interactions are included in the calculations.

The region from 1500 to 1350 $cm^{-1}$ contains six bend modes of the methyl groups and one bend mode of the methylene group. The calculated frequencies in this region fit the observed data satisfactorily. The PEDs show that the $\alpha$-$CH_3$ asymmetric bend 1 mixes with the $CH_2$ bend mode; all other methyl bends are well localized. The dispersion curves are essentially flat in this region. The bands in the region from 1350 to 1300 correspond to the $CH_2$ wag mode with considerable contributions from the backbone and side-chain CC stretch vibrations. The infrared bands in this region exhibit crystallization-sensitive behavior.[11]

The region from 1300 to 1050 $cm^{-1}$ consists of mixed modes that are highly coupled along the chain, as indicated by the dispersion curves. This may account for

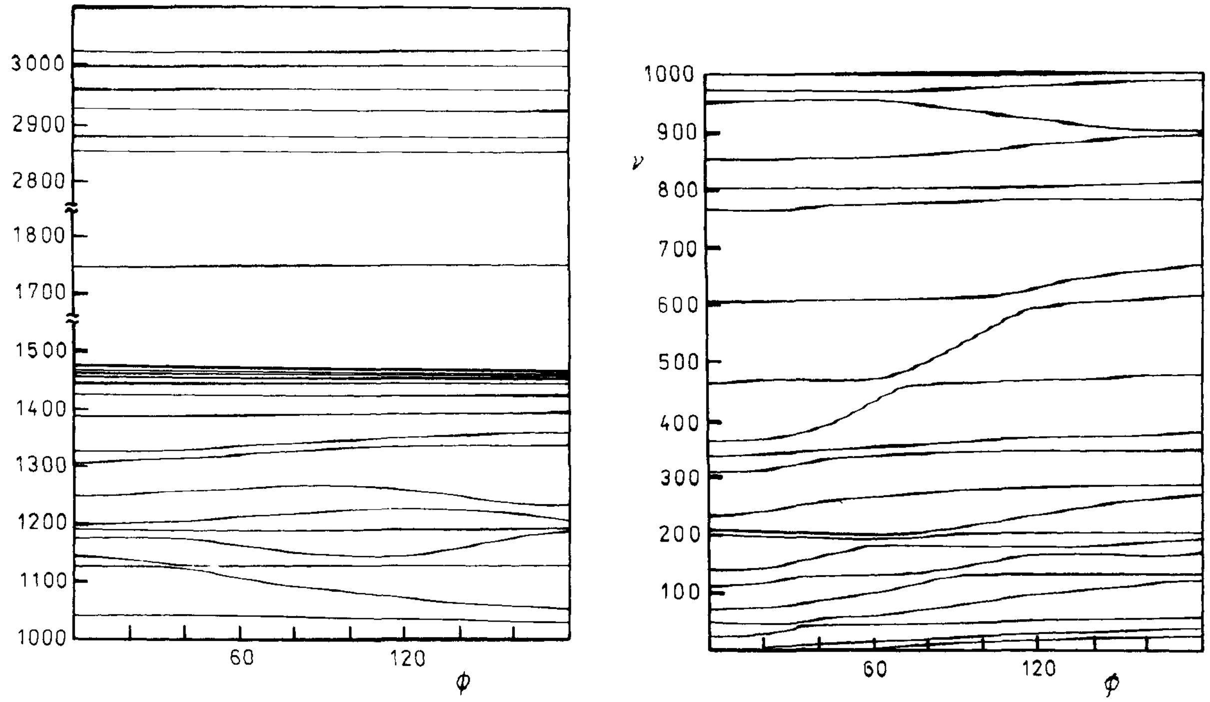

**Figure 4.** Dispersion curves for the single 10/1 i-PMMA chain.

some large discrepancies between observed and calculated frequencies, which would be sensitive to small changes in (presently unrefined) interaction force constants. The distinctive $E_2$ species C–O stretch + $CH_2$ twist mode at 1231 $cm^{-1}$ is well predicted, as are the mixed modes with $OCH_3$ rock in the 1210–1190 $cm^{-1}$ region. The observed band pattern in the 1160–1100 $cm^{-1}$ region is reasonably well reproduced, except for the $E_1$ species mode calculated at 1177 $cm^{-1}$. As can be seen, the $OCH_3$ rock mode calculated at 1129 $cm^{-1}$ completely changes its character in the A species vibration at 1147 $cm^{-1}$.

The bands near 998 $cm^{-1}$ in the infrared and Raman spectra have been assigned to the $OCH_3$ rock vibration interacting with the stretch vibrations of the COC group.[2,6] Though this assignment is essentially confirmed by the normal coordinate calculations, the PED indicates large contributions from the O–C stretch vibration. As can be seen from Table IV, the observed frequencies of these modes are not well reproduced. Calculations show that the fit can be improved considerably by refinement of the *f*(C–O,O–C) force constant, without any practical change in the character of the vibration. However, since we decided to adhere strictly to transferability of force fields, we did not undertake this refinement. (In any case, it should properly be done only with the incorporation of the correct nontetrahedral geometry.) The observed weak band in the infrared spectrum with A component at 1058 $cm^{-1}$ and $E_1$ component at 1064 $cm^{-1}$ is not predicted by the normal-mode calculations. Since it appears also in the infrared spectrum of amorphous i-PMMA (at 1061 $cm^{-1}$), it is not a crystallinity-sensitive band. We suppose that this band belongs to a combination, probably 602 (A) + 467 (A) = 1069 (A) and 603 ($E_1$) + 467 (A) = 1070 ($E_1$).

Two $\alpha$-$CH_3$ rock modes appear between 960 and 930 $cm^{-1}$, in agreement with the previous assignments.[2,6] (The weak perpendicular band at 980 $cm^{-1}$ may be a combination: 602 (A) + 380 ($E_1$) = 982 ($E_1$).) The $\alpha$-$CH_3$ rock mode at the lower frequency is coupled with the mixed vibration having A component near 850 $cm^{-1}$. This is illustrated by the corresponding dispersion curves, which closely approach each other at high-phase angles. The characteristic band of the crystalline phase of i-PMMA found at 882 $cm^{-1}$ in the infrared spectrum[11] is not predicted as a fundamental by the present normal-mode calculations. Its parallel character may be due to a combination band: 770 (A) + 110 (A) = 880 (A).

On the basis of the infrared and Raman spectra of i-PMMA, the bands observed near 760 $cm^{-1}$ were assigned to the $CH_2$ rock mode[2] or to skeletal vibrations,[4] probably affected by the $CH_2$ rock vibration.[6] However, the calculated PED indicates that these modes contain predominantly C═O out-of-plane bend with contributions of side-chain bend motions. In the Raman spectra, a doublet occurs at 597 and 562 $cm^{-1}$ and this doublet remains essentially unchanged during the transition of the i-PMMA sample from the unordered to the ordered state (Figure 2). According to the normal coordinate calculations, only one mode, $C^{\alpha}C^{*}$ stretch combined with C═O in-plane bend, is predicted in this frequency region. It is possible that the doublet is due to a Fermi resonance between the fundamental and a combination mode with components in the Raman: 372 (A) + 221 (A) = 593 (A). This is reasonable, since the fundamentals all involve motions essentially localized in the C–CO–O group (cf. PEDs in Table IV). It is interesting to note that a similar explanation can account for the doublet in the perpendicularly polarized infrared spectrum at 609 and 559 $cm^{-1}$: 372 (A) + 232 ($E_1$) = 604 ($E_1$). If, as observed in Figure 3, the two bands are of about the same intensity, the unperturbed fundamental would be at 584 $cm^{-1}$, diminishing the discrepancy with the calculated band.

As can be seen from Table IV, the low-frequency part of the vibrational spectrum contains several highly mixed modes. These modes are mainly due to the backbone and the ester group bend and, in the region below 230 $cm^{-1}$, significant contributions from six torsions. The dispersion curves indicate a great deal of coupling between the modes in the whole region below 700 $cm^{-1}$. While the frequency agreement in this region is not particularly good, the pattern of assignments is quite reasonable.

## Conclusions

A comparison of observed low-frequency infrared and Raman bands with frequencies calculated for the 5/1 and 10/1 helix chain conformations of i-PMMA clearly favors the latter structure. The calculations on the 10/1 structure reproduce the overall frequencies fairly well, the average discrepancy between observed and calculated frequencies being 11.6 $\mathrm{cm}^{-1}$. This is despite the assumption of a standard geometry for the backbone and the transfer without refinement of main-chain and side-chain force constants from hydrocarbons and methyl acetate. The calculated PEDs and dispersion curves provide insight into the vibrational behavior of the i-PMMA chains.

These calculations have been performed on a simple model structure of crystalline i-PMMA, i.e., the regular single 10/1 helix with parallel ester groups in a trans orientation. Energy calculations[23,24] indicate that interactions can lead, for example, to the stabilization of the antiparallel arrangement of the successive ester groups. Before such details of the conformational structure of i-PMMA can be analyzed by normal-mode calculations, further refinement of the force field, using isotopic derivatives and the observed chain geometry, is necessary. The present analysis provides a persuasive starting point for such a study.

**Acknowledgment.** This research was supported by S. C. Johnson and Son, Inc., and by NSF Grant DMR-8806975.

## References and Notes

(1) Baumann, U.; Schreiber, H.; Tessmar, K. *Makromol. Chem.* **1960**, *36*, 81.
(2) Nagai, H. *J. Appl. Polym. Sci.* **1963**, *7*, 1697.
(3) Havriliak, S.; Roman, N. *Polymer* **1966**, *7*, 387.
(4) Willis, H. A.; Zichy, V. J. I.; Hendra, P. *Polymer* **1969**, *10*, 737.[1]
(5) Tadokoro, H.; Chatani, Y.; Kusanagi, H.; Yokoyama, M. *Macromolecules* **1970**, *3*, 441.
(6) Schneider, B.; Štokr, J.; Schmidt, P.; Mihajlov, P.; Dirlikov, S.; Peeva, N. *Polymer* **1979**, *20*, 705.
(7) Dirlikov, S. K.; Koenig, J. L. *Appl. Spectrosc.* **1979**, *33*, 555.
(8) O'Reilly, J. M.; Mosher, R. A. *Macromolecules* **1981**, *14*, 602.
(9) Dybal, J.; Štokr, J.; Schneider, B. *Polymer* **1983**, *24*, 971.
(10) Spěváček, J.; Schneider, B.; Dybal, J.; Štokr, J. *Croat. Chem. Acta* **1987**, *60*, 11.
(11) Schneider, B.; Štokr, J.; Spěváček, J.; Baldrian, J. *Makromol. Chem.* **1987**, *188*, 2705.
(12) de Boer, A.; van Ekenstein, A.; Challa, G. *Polymer* **1975**, *16*, 930.
(13) Könnecke, K.; Rehage, G. *Colloid Polym. Sci.* **1981**, *259*, 1062.
(14) Snyder, R. G.; Schachtschneider, J. H. *Spectrochim. Acta* **1965**, *21*, 169.
(15) Dybal, J.; Krimm, S. *J. Mol. Struct.* **1988**, *189*, 383.
(16) Stroupe, J. D.; Hughes, R. E. *J. Am. Chem. Soc.* **1958**, *80*, 2341.
(17) Coiro, V. M.; DeSantis, P.; Liquori, A. M.; Mazzarella, L. *J. Polym. Sci., Part C* **1969**, *16*, 4591.
(18) Tadokoro, H.; Tai, K.; Yokoyama, M.; Kobayashi, M. *J. Polym. Sci., Polym. Phys. Ed.* **1973**, *11*, 825.
(19) Kusanagi, H.; Tadokoro, H.; Chatani, Y. *Macromolecules* **1976**, *9*, 531.
(20) Coiro, V. M.; Liquori, A. M.; De Santis, P.; Mazzarella, L. *J. Polym. Sci., Polym. Lett. Ed.* **1978**, *16*, 33.
(21) Lovell, R.; Windle, A. H. *Macromolecules* **1981**, *14*, 211.
(22) Sundararajan, P. R. *Macromolecules* **1979**, *12*, 575.
(23) Vacatello, M.; Flory, P. J. *Polymer Commun.* **1984**, *25*, 258.
(24) Vacatello, M.; Flory, P. J. *Macromolecules* **1986**, *19*, 405.
(25) Bosscher, F.; ten Brinke, G.; Eshius, A.; Challa, G. *Macromolecules* **1982**, *15*, 1364.
(26) Snyder, R. G. *J. Chem. Phys.* **1967**, *47*, 1316.
(27) Moore, W. H.; Krimm, S. *J. Mol. Spectrosc.* **1974**, *51*, 1.
(28) Krimm, S.; Bandekar, J. *Adv. Protein Chem.* **1986**, *38*, 181.
(29) Loutfy, R. O.; Teegarden, D. M. *Macromolecules* **1983**, *16*, 452.
(30) Van Alsenoy, C.; Scarsdale, J. N.; Schäfer, L. *J. Mol. Struct.* **1982**, *90*, 297.
(31) Dybal, J.; Spěváček, J.; Schneider, B. *J. Polym. Sci., Polym. Phys. Ed.* **1986**, *24*, 657.
(32) Dwivedi, A. M.; Krimm, S.; Malcolm, B. R. *Biopolymers* **1984**, *23*, 2025.
(33) Snyder, R. B.; Hsu, S. L.; Krimm, S. *Spectrochim. Acta* **1978**, *34A*, 395.
(34) Krimm, S.; Abe, Y. *Proc. Natl. Acad. Sci.* **1972**, *69*, 2788.
(35) Krimm, S. *Biopolymers* **1983**, *22*, 217.
(36) Cheam, T. C.; Krimm, S. *Chem. Phys. Lett.* **1984**, *107*, 613.
(37) Dybal, J.; Cheam, T. C.; Krimm, S. *J. Mol. Struct.* **1987**, *159*, 183.

**Registry No.** i-PMMA, 25188-98-1.